Magnetic-field-induced Fabry-Pérot resonances in helical edge states

Abhiram Soori,[1] Sourin Das,[2] and Sumathi Rao[3]
[1]*Centre for High Energy Physics, Indian Institute of Science, Bangalore 560012, India*
[2]*Department of Physics and Astrophysics, University of Delhi, Delhi-110 007, India*
[3]*Harish-Chandra Research Institute, Chhatnag Road, Jhusi, Allahabad 211 019, India*
(Received 13 January 2012; revised manuscript received 23 August 2012; published 17 September 2012)

We study electronic transport across a helical edge state exposed to a uniform magnetic ($\vec{B}$) field over a finite length. We show that this system exhibits Fabry-Pérot-type resonances in electronic transport. The intrinsic spin anisotropy of the helical edge states allows us to tune these resonances by changing the direction of the $\vec{B}$ field while keeping its magnitude constant. This is in sharp contrast to the case of nonhelical one-dimensional electron gases with a parabolic dispersion, where similar resonances do appear in individual spin channels ($\uparrow$ and $\downarrow$) separately which, however, cannot be tuned by merely changing the direction of the $\vec{B}$ field. These resonances provide a unique way to probe the helical nature of the theory. We study the robustness of these resonances against a possible static impurity in the channel.

DOI: 10.1103/PhysRevB.86.125312 PACS number(s): 73.23.−b, 71.10.Pm, 73.63.Nm

I. INTRODUCTION

Edge states of a new class of insulators called topological insulators form an interesting class of one-dimensional (1D) systems called helical edge states (HES).[1] The central feature of these edge states is the fact that the direction of propagation of the quasiparticles is directly correlated with their spin projection; i.e., counterpropagating particles have opposite spin projections. Various aspects of this state have been studied.[2] Experimental evidence has been found for the existence of these edge states in a multiterminal Hall bar setup.[3]

The fact that the spin of the electrons can be controlled and manipulated by manipulating its momentum due to spin-momentum locking has generated great interest in the possible application of HES to the field of spintronics.[4] Besides electrical control, it is interesting to study the possibility of controlling the spin of electrons on such edge states using magnetic fields. This could be of great interest from the point of view of application to spintronic devices. Since spin-rotation symmetry is strongly broken in such edge states, a strong anisotropic response to an applied magnetic field is expected, and the edge gaps have been computed.[3] Hence one of the more intriguing features of the HES as opposed to the usual one-dimensional electron gas with parabolic dispersion lies in its response to magnetic fields. Naively, introduction of a magnetic field breaks the time-reversal symmetry which is central to the topological stability of the quantum Hall insulators which hosts these HES on its boundary. There have been studies[5] of some aspects of minimal coupling of the four-band model[1] to a magnetic field. However, it is still of interest to study the response of the HES to small magnetic fields which do not significantly disturb the bulk stability of the topological insulators but do influence the edge states in a nontrivial way.

From the viewpoint of device applications, the study of tunneling across barriers or backscattering from tunnel barriers implanted on the edge states is of central interest as they can act as experimentally tunable quantum resistors, which are essential elements of any quantum circuitry. A simple way to produce controlled backscattering in mesoscopic devices is to apply local gate voltages. But for HES such techniques are not effective because all electrical barriers are rendered transparent due to Klein tunneling of massless Dirac electrons. Further, protection of HES against inelastic backscattering due to electron-phonon coupling has also been reported.[6] Hence, an alternate way is needed to produce backscattering, and therefore magnetic barriers which do give rise to backscattering are of vital importance. Transmission through magnetic barriers has been studied in the case of chiral modes in carbon nanotubes[7] and surface states of three-dimensional (3D) topological insulators;[8] however, a similar study for HES is lacking, and such a study is the central focus of this paper. Also, recently, there have been theoretical studies involving spin-polarized scanning tunneling microscopy (STM) as a direct probe for testing the theoretical prediction of the helical nature of the surface states, both in the context of two-dimensional (2D) and 3D topological insulators.[9] Experimentally, only very recently,[10] the spin polarization at the edge was studied purely by electrical means; hence such proposals are of crucial importance. Here, we propose yet another way to probe the helical nature of HES.

In this paper, we study the effect of a magnetic field patch on edge-state transport. As shown in Ref. 3, we find that any $\vec{B}$ field with a nonzero component in the plane perpendicular to the spin-quantization axis of left- and right-moving states opens up a gap in the spectrum. Further, the spin of the left- and right-moving states gets twisted. In other words, even in the presence of the $\vec{B}$ field, the direction of motion remains tied with its spin; however, unlike in free HES, the counterpropagating states no longer have spins antiparallel to each other. We show that these states in the $\vec{B}$-field patch induce Fabry-Pérot-type resonances in transport across the patch which are tunable purely by changing the direction of the $\vec{B}$ field. The resonances hence provide a direct way to quantify the degree of spin anisotropy in these systems.

II. THE MODEL AND ANALYSIS

Consider a smooth infinitely extended helical edge state exposed to a uniform $\vec{B}$ field over a finite length L described

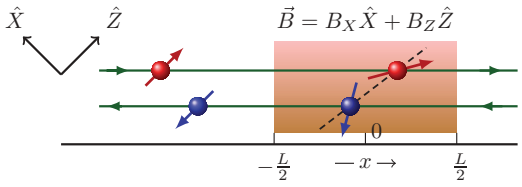

FIG. 1. (Color online) Schematic of the model. Shaded region $|x| < L/2$ is the region of constant magnetic field $\vec{B}$. Spin orientations of the left (right) moving modes are tilted by B_X in the clockwise (counterclockwise) direction by the same angle.

by the following Hamiltonian:[1]

$$H_0 = -i\hbar v_F \int dx \psi^\dagger(x)\sigma_z\partial_x\psi(x), \tag{1}$$

where $\psi = [\psi_{R\uparrow}\psi_{L\downarrow}]^T$ and the R/L index corresponds to right and left movers. x parameterizes the coordinate along the 1D edge state. X,Y,Z are chosen to describe the spin such that Z points along the spin-quantization axis of right-moving eigenstates in the absence of $\vec{B}$ field, and X is chosen to be along the component of applied $\vec{B}$ in the plane perpendicular to Z.[11] Since it is redundant, we will henceforth drop the L/R indices in $\psi_{L/R\sigma}$. We now introduce a uniform magnetic field in the region $|x| < L/2$ (sketched in Fig. 1). The Zeeman coupling of the magnetic field to the intrinsic spin of the electrons can be modeled by

$$H_B = g\mu_B \int dx \Delta_L(x)\vec{S}(x)\cdot\vec{B}, \tag{2}$$

where $\Delta_L(x) = [\Theta(x + L/2) - \Theta(x - L/2)]$, $\vec{S}(x) = 1/2[\psi^\dagger(x)\,\vec{\sigma}\,\psi(x)]$ is the spin operator, g is the g factor of the electron, and μ_B is the Bohr magneton. The corresponding Heisenberg equations of motion for the fields $\psi(x,t)$ is given by

$$i\hbar\partial_t\psi = \left[-i\hbar v_F\sigma_z\partial_x + \frac{g}{2}\mu_B\Delta_L(x)\vec{\sigma}\cdot\vec{B}\right]\psi. \tag{3}$$

By rescaling the energy $E \rightarrow E/W$ and by defining the dimensionless variables $x \rightarrow \bar{x} = xW/\hbar v_F$, $B \rightarrow \bar{B} = \mu_B B/W$, and $k \rightarrow \bar{k} = \hbar v_F k/W$, where W is the bulk gap, we can rewrite this equation in terms of dimensionless variables as $\bar{E}\psi = [-i\sigma_z\partial_{\bar{x}} + \frac{g}{2}\Delta_L(\bar{x})\vec{\sigma}\cdot\vec{B}]\psi$. We will henceforth drop the bars.

A. Magnetic field twists helicity

The Hamiltonian given in Eq. (1) describing free edge-state electrons is time-reversal symmetric. But the Zeeman-coupling term H_B in Eq. (2) breaks time-reversal symmetry and opens up a gap in the spectrum. In regions of zero magnetic field we know that the up spin (pointing along the $+Z$ direction) moves right and the down spin (pointing along the $-Z$ direction) moves left. But in the region with nonzero magnetic field, this is no longer true; still, the direction of motion is correlated to the spin orientation for propagating states above and below the gap. To look for the eigenstates of the Hamiltonian $H_0 + H_B$, in the region $|x| < L/2$, we start with a plane-wave solution $\psi_k e^{i(kx-\omega t)}$, where ψ_k is

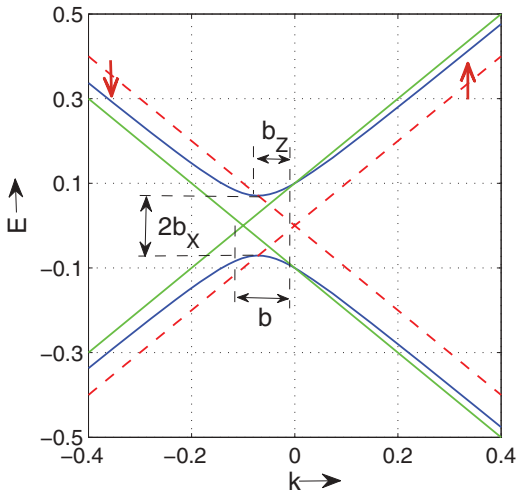

FIG. 2. (Color online) Blue (dark gray) and green (light gray) solid curves stand for schematic dispersions when the $\vec{B}$ field is at angles $\phi = \pi/4$ and $\phi = 0$ with the positive Z axis, respectively. $b = |\vec{b}| = 0.1$ in both cases. Red dashed curve corresponds to the zero-field case.

the Fourier transform of the spinor field $\psi(x)$. Substituting the above form into Eq. (3), we find the dispersion relation to be $E = \pm\sqrt{\tilde{k}^2 + b_x^2}$, where $b_X = gB_X/2$, $b_z = gB_z/2$, and $\tilde{k} = k + b_z$. Thus, the spectrum is gapped for nonzero B_X with a gap given by b_X, and the spectrum breaks into two bands.

The magnetic field $\vec{B}$ can be, in general, at an angle ϕ with the Z axis i.e., $\vec{b} = b(\sin\phi\hat{X} + \cos\phi\hat{Z})$. The dispersion relation for the three different cases corresponding to $\vec{b} = 0$ and directions $\phi = 0$ and $\phi = \pi/4$ with nonzero b is shown in Fig. 2. Note that in the presence of a finite $\vec{B}$ field, the $k = 0$ states are split exactly by $2b_X$, as expected for spin half particles with zero momentum.

At a given energy E there are two eigenstates (right and left moving) $\psi_{E,R/L}$ with momenta $k = k_R$ and $k = -k_L$, respectively, given by

$$\begin{aligned}\psi_{E,R} &= \frac{1}{N}[E + \tilde{k}_0 b_X]^T; \quad \psi_{E,L} = \sigma_x\psi_{E,R},\\ k_{R/L} &= \left[\mp b_z + \mathrm{sgn}(E)\sqrt{E^2 - b_x^2}\right],\end{aligned} \tag{4}$$

where N is the normalization and $\tilde{k}_0 = (k_R + k_L)/2$. Here, each state ψ_E has its spin pointing in a distinct direction, and the left- and right-moving modes are no longer antiparallel. At a given energy E (not in the gap, i.e., $|E| < |b_x|$), we find the spin orientation $\vec{S}_P = \langle\psi_P\,|\,\vec{S}\,|\,\psi_P\rangle$ for the right/left movers ($P = R/L$), where $\vec{S} = \vec{\sigma}/2$ is the spin operator, to be given by $S_{R/L} = (b_x, 0, \pm\tilde{k}_0)/2E$. When $|E| \gg |b_x|$, the spin for the R/L movers points along the $Z/-Z$ direction, as expected. Also, note that the states at the bottom of the upper band and the top of lower band are located at $k = -b_z$, which implies that $\tilde{k}_0 = 0$; here, the respective spins point parallel and antiparallel to the X axis. For this value of the momentum, the momentum-dependent pseudomagnetic field acting on the electron due to the helical nature of the free Hamiltonian is fully canceled by the Z component of the applied magnetic

field; hence it leaves behind a net $\vec{B}$ field pointing along the X direction.[12] More generally, in a given band, left-moving and right-moving modes with the same energy are twisted by the magnetic field component B_x by the same angle but in opposite directions, as sketched in Fig. 1.

B. Transmission through the magnetic patch

Consider the case where an electron is incident on the $\vec{B}$-field patch from the left with an energy E_i and momentum $k_i = E_i$. Then the corresponding left- and right-moving momentum eigenstates that the incident particle excites in the patch region can be read off from Eq. (4) with $E = E_i$. The scattering states in different regions are given by

$$\psi = \begin{cases} |\uparrow\rangle\, e^{ik_i x} + r_{k_i}|\downarrow\rangle\, e^{-ik_i x} & \text{for} \quad x < -L/2, \\ A_R\, \psi_{E_i R}\, e^{ik_R x} + A_L\, \psi_{E_i L}\, e^{-ik_L x} & \text{for} \quad |x| < L/2, \\ t_{k_i}\, e^{ik_i x}|\uparrow\rangle & \text{for} \quad x > L/2, \end{cases} \tag{5}$$

where $|\uparrow\rangle$ and $|\downarrow\rangle$ are eigenstates of σ_z, r and t are the reflection and the transmission amplitudes, and A_L and A_R are the amplitudes corresponding to the left- and right-moving eigenstates in the $\vec{B}$-field patch. Using appropriate boundary conditions, we get the following expression for transmission amplitude:

$$t_{k_i} = \frac{\tilde{k} e^{-i(k_i + b_z)L}}{\tilde{k}\cos[\tilde{k}L] - i k_i \sin[\tilde{k}L]}. \tag{6}$$

Note that the resonance corresponds to $(k_R + k_L)L = 2n\pi$, which is the total phase picked up by the electron in one round trip journey across the $\vec{B}$ field patch, i.e., very similar to the double barrier resonance. However, as we shall see, the dynamics of the spin in the $\vec{B}$ field is very different. The most interesting point to note here is the fact that the resonance condition does not depend on $|\vec{B}|$ but only on B_x. Hence the resonances can be tuned simply by rotating the $\vec{B}$ field away or toward the Z axis without changing its magnitude. This observation is the central message of this paper. A plot of the transmission probability at fixed k_i, which is the differential conductance in units of e^2/h evaluated at fixed bias, corresponding to an electron incident with energy E_i from the left reservoir while the right reservoir is held at zero potential, is shown as a function of ϕ in Fig. 3, inset (a). As we can see from Fig. 3, inset (a), the conductance shows sharp resonances as we vary ϕ for $L = 100$. The resonances get sharper as b_x approaches E_i from $b_x = 0$, and beyond E_i, transport is subgapped. On the other hand, for a short $\vec{B}$-field patch [$L = 10$ in Fig. 3, inset (a)], the transport is nonresonant, but the differential conductance can be as large as $0.1e^2/h$ in the subgapped regime ($\phi > 0.3\pi$). Further we study the case of a more realistic $\vec{B}$-field patch wherein magnetic field changes from zero to maximum smoothly over a length scale ξ, as illustrated in Fig. 3, inset (b). We calculate the transmission amplitude for such a magnetic field profile numerically using the transfer-matrix method. The helical edge is sliced into a large number of segments N_L, where the magnetic field is taken to be uniform in each segment. Then, the wave function is written in each segment similar to that given in Eq. (5). Matching ψ at the boundaries of the segments gives the

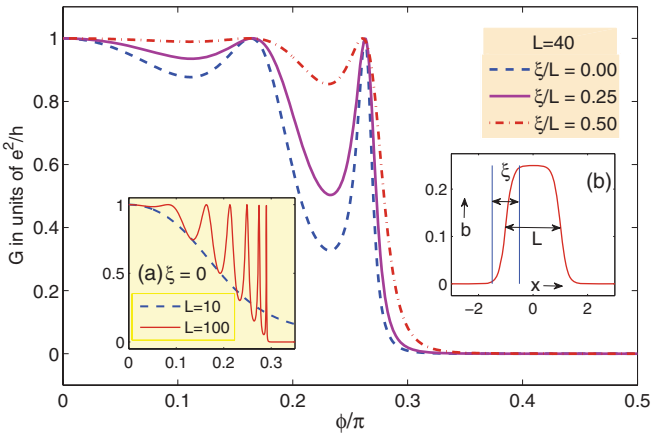

FIG. 3. (Color online) Differential conductance G vs angle ϕ for different ξ/L. Inset (a): G vs ϕ for two different lengths of the patch with $\xi = 0$. Inset (b): Illustration of how $b = |\vec{b}|$ changes across the patch for a fixed ϕ. Parameters $b_0 = \max\{|\vec{b}|\} = 0.25$ and $E_i = 0.2$ are the same in all the plots.

transmission amplitude. We see from the main part of Fig. 3 that the visibility of the resonances is affected by increasing ξ. However, even the least visible first resonance (around $\phi = 0.18\pi$), which is most affected by increasing ξ, is still visible for ξ/L in the range (0,0.25).

C. Spin orientation in the magnetic patch

In the patch, the Zeeman term H_B competes with the kinetic-energy term H_0 and twists the spin directions of left/right movers $\psi_{E_i L/R}$ (as pictured in Fig. 1). Hence, due to the mismatch in spin orientation, an electron incident on the patch typically undergoes multiple reflections in the patch. Thus, the spin density at any point in the patch has contributions from both $\psi_{E_i L}$ and $\psi_{E_i, R}$. Evaluating the spin density $\langle\psi|\vec{\sigma}/2|\psi\rangle$ in the patch using the wave functions given in Eq. (5), we find that $\vec{S}_k(x)$ at any point x makes a constant angle with the axis $\vec{n}_k = (b_x, 0, k)(1/\sqrt{k^2 + b_x^2})$. Hence, $\vec{n}_k$ defines the direction of the effective magnetic field around which the spin density precesses. This precession is quite

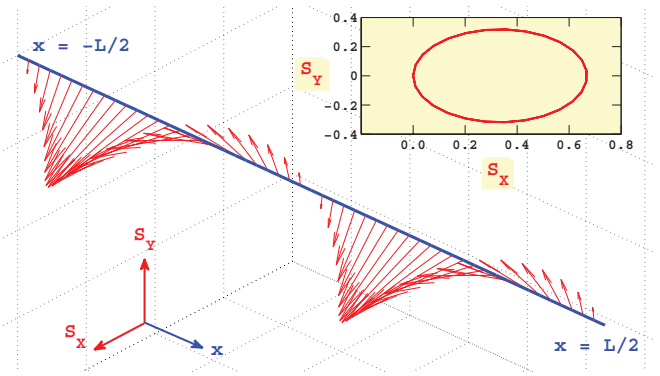

FIG. 4. (Color online) X and Y components of spin density at different points in the magnetic patch for resonant transport $b_x = 0.1$, $b_z = 0$, $L = 180$, $E_i = 0.0366$. The inset shows S_x and S_y at different values of x; $S_y = 0$ at $x = -L/2, -L/4, 0, L/4, L/2$, while $S_x = 0$ at $x = -L/2, 0, L/2$.

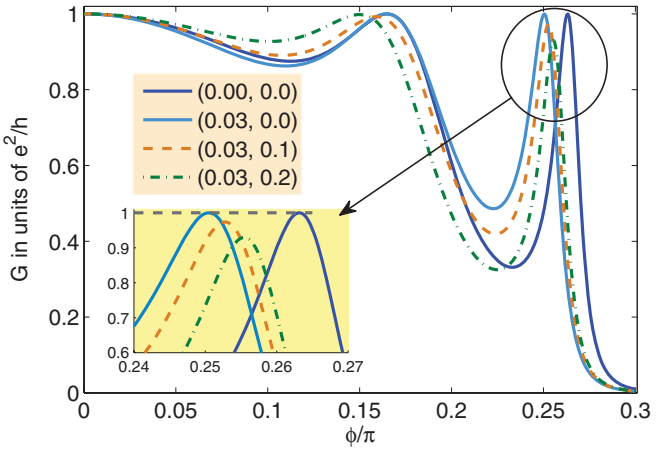

FIG. 5. (Color online) Illustration of change in visibility of resonances due to disorder of strength $\eta = 0.03$ in the patch. Parameters chosen are same as those in Fig. 3, except $\xi/L = 0.05$, $l/L = 0.1$. The legend shows $(\eta, x_l/L)$ for different curves.

novel: the component of the spin vector along the precession axis $\vec{n}_k$ varies as the spin precesses, whereas the component along the Z axis is conserved, compared to the usual case where the component along the precession axis is conserved. For a resonant case (an example is shown in Fig. 4), $\vec{S}_{k_i} = \hat{Z}/2$ at both $L/2$ and $-L/2$. In other words, the angle of precession of the electron across the patch is an exact integer multiple of 2π, similar to the operational principle of the Datta-Das transistor.[13] Thus, the resonance condition is directly coupled to evolution of the spin density along the $\vec{B}$-field patch. This implies that our setup can be regarded as a possible candidate for devising a spin transistor.

III. CONDITIONS FOR EXPERIMENTAL OBSERVATION

(i) Our calculation inherently assumes that the helical edge has a finite $\vec{B}$-field patch and reservoirs are away from this patch.

(ii) The ratio ξ/L has to be small. $\xi/L < 0.25$ would be a reasonable limit for a typical case, as mentioned earlier.

(iii) The magnetic field that opens up a gap in the spectrum should not force the edge states to tunnel into the bulk. This means that the gap opened on the edge by $\vec{B}$ field should be less than bulk gap ($2|b_x| < 1$) and the energy of the incident electron should also be within the bulk gap ($|E_i| < 1/2$). A limit on the magnetic field then can be estimated to be 7 T.[14]

(iv) *Coherence*. A realistic sample can have inelastic backscattering[3] on the edge, which causes spin decoherence. Since resonance is an interference phenomenon, it is essential that spin-decoherence length $l_d \gg L$.[15]

(v) *Disorder*. The topological protection against backscattering due to scalar impurities breaks down in the presence of the time-reversal-breaking magnetic field. Hence one cannot naively throw away the disorder term. In a good sample we expect the disorder to be weak and sparsely spaced and to have a length scale $l \ll L$. Such an impurity can be modeled by a rectangular potential barrier/well with width l and height η. This impurity may be centered anywhere ($|x_l| < L/2$) in the magnetic field patch. We have studied the effect of such an impurity with a fixed l with different disorder strengths η, positioned across the patch ($|x_l| < L/2$). We find that as long as $|\eta| \ll |E_i|$, the resonances are not affected. We have given an illustrative plot in Fig. 5 of how the resonances are affected for a value of $\eta/E_i = 0.15$ positioned in the patch.[16]

IV. DISCUSSION AND CONCLUSION

The most crucial element involved in devising the proposed setup is to realize the localized $\vec{B}$-field patch whose direction should be fully tunable. In Ref. 3, the effect of the magnetic anisotropy on the suppression of the quantum spin Hall effect was studied, and the gaps induced by the perpendicular and in-plane fields were obtained. Here, we require a localized $\vec{B}$-field patch, which should be possible to engineer using the proximity effect[17] by depositing a layer of magnetic material on top of the edge. Moreover, by choosing a magnetic material which shows current-induced rotation of magnetization,[18] it should be possible to rotate the direction of the $\vec{B}$ field in the patch. Further, since spin coherence is essential to observe resonances, spin decoherence arising from any mechanism other than inelastic backscattering reported in Ref. 3 can be probed in the proposed setup. So, in conclusion, we have discussed a concrete proposal to probe the degree of spin anisotropy in the HES via the Fabry-Pérot resonances. Note that similar surface states appear in 3D topological insulators, and the extent to which such states are helical (spin-momentum locked) is not yet fully understood. Also, these have been probed not via direct transport experiments but via optics experiments, such as spin-resolved angle-resolved photoemission spectroscopy, which see a deviation[19] from the purely theoretical picture of the 2D helical surface states. Hence in the context of 2D topological insulators where 1D HES appear on the boundary, studying these resonances could lead to crucial information and characterization of deviations from the theoretically predicted helical nature, if any. Also, as an application, our setup provides a possible design for a resonant spin transistor.

ACKNOWLEDGMENTS

We thank Diptiman Sen, Amir Yacoby, and Yuval Oreg for stimulating discussions. A.S. thanks HRI and DU for kind hospitality during the stay and CSIR, India, for financial support. S.R. thanks ICTS, Bangalore, for kind hospitality during the completion of this work.

[1]C. L. Kane and E. J. Mele, Phys. Rev. Lett. **95**, 226801 (2005); **95**, 146802 (2006); B. A. Bernevig, T. L. Hughes, and S. C. Zhang, Science **314**, 1757 (2006); M. Buttiker, *ibid.* **325**, 278 (2009); M. Z. Hasan and C. L. Kane, Rev. Mod. Phys. **82**, 3045 (2010); X.-L. Qi and S.-C. Zhang, *ibid.* **83**, 1057 (2011).

[2]C. Wu, B. A. Bernevig, and S. C. Zhang, Phys. Rev. Lett. **96**, 106401 (2006); C.-Y. Hou, E.-A. Kim, and C. Chamon, *ibid.* **102**, 076602 (2009); J. Maciejko, C. Liu, Y. Oreg, X.-L. Qi, C. Wu, and S. C. Zhang, *ibid.* **102**, 256803 (2009); A. Ström and H. Johannesson, *ibid.* **102**, 096806 (2009); A. Bermudez, D. Patane, L. Amico, and M. A. Martin-Delgado, *ibid.* **102**, 135702 (2009); J. E. Moore, Nature (London) **464**, 194 (2010); N. Goldman, I. Satija, P. Nikolic, A. Bermudez, M. A. Martin-Delgado, M. Lewenstein, and I. B. Spielman, Phys. Rev. Lett. **105**, 255302 (2010); R. Egger, A. Zazunov, and A. Levy Yeyati, *ibid.* **105**, 136403 (2010); P. Virtanen and P. Recher, Phys. Rev. B **83**, 115332 (2011).

[3]M. König, H. Buhmann, L. W. Molenkamp, T. L. Hughes, C.-X. Liu, X.-L. Qi, and S.-C. Zhang, J. Phys. Soc. Jpn. **77**, 031007 (2008); M. König, S. Wiedmann, C. Brüne, A. Roth, H. Buhmann, L. Molenkamp, X.-L. Qi, and S.-C. Zhang, Science **318**, 766 (2007).

[4]J. Maciejko, E.-A. Kim, and X.-L. Qi, Phys. Rev. B **82**, 195409 (2010).

[5]G. Tkachov and E. M. Hankiewicz, Phys. Rev. Lett. **104**, 166803 (2010).

[6]J. C. Budich, F. Dolcini, P. Recher, and B. Trauzettel, Phys. Rev. Lett. **108**, 086602 (2012).

[7]A. V. Parafilo, I. V. Krive, E. N. Bogachek, U. Landman, R. I. Shekhter, and M. Jonson, Low Temp. Phys. **36**, 959 (2010); Phys. Rev. B **83**, 045427 (2011).

[8]S. Mondal, D. Sen, K. Sengupta, and R. Shankar, Phys. Rev. Lett. **104**, 046403 (2010).

[9]S. Das and S. Rao, Phys. Rev. Lett. **106**, 236403 (2011); K. Saha, S. Das, K. Sengupta, and D. Sen, Phys. Rev. B **84**, 165439 (2011).

[10]C. Brüne, A. Roth, H. Buhmann, E. M. Hankiewicz, L. W. Molenkamp, J. Maciejko, X.-L. Qi, and S.-C. Zhang, Nat. Phys. **8**, 486 (2012).

[11]We have ignored the orbital coupling to B_Z and the consequent breaking of S_Z symmetry. A more complete treatment is under preparation.

[12]M. Kharitonov, arXiv:1004.0194.

[13]S. Datta and B. Das, Appl. Phys. Lett. **56**, 665 (1990).

[14]For HgTe, $g \sim 50$ [M. V. Yakunin, S. M. Podgornykh, N. N. Mikhailov, and S. A. Dvoretsky, Physica E **42**, 948 (2010)] and bulk-gap $\sim$0.02 eV (X.-L. Qi *et al*. in Ref. 1).

[15]In HgTe quantum wells, the inelastic mean free path has been reported to be around 1 μm (Ref. 3).

[16]A more detailed analysis of disorder is under preparation.

[17]R. J. Epstein, I. Malajovich, R. K. Kawakami, Y. Chye, M. Hanson, P. M. Petroff, A. C. Gossard, and D. D. Awschalom, Phys. Rev. B **65**, 121202(R) (2002).

[18]V. Uhlir, J. Vogel, N. Rougemaille, O. Fruchart, Z. Ishaque, V. Cros, J. Camarero, J. C. Cezar, F. Sirotti, and S. Pizzini, J. Phys. Condens. Matter **24**, 024213 (2012).

[19]Z.-H. Pan, E. Vescovo, A. V. Fedorov, D. Gardner, Y. S. Lee, S. Chu, G. D. Gu, and T. Valla, Phys. Rev. Lett. **106**, 257004 (2011).